Geotechnical Reconnaissance and Engineering Effects of the December 29, 2020, M6.4 Petrinja, Croatia Earthquake, and Associated Seismic Sequence

Chapter 5: Surface Deformations

Authors: Marin Govorčin, Dellena Kinikles

5 Surface Deformation

5.1 Surface Deformations

Interferometric Synthetic Aperture Radar (InSAR) was used to analyze the ground surface deformations induced by the Dec. 29, 2020 M_w 6.4 Petrinja Earthquake. The technique measures ground surface displacements by comparing radar imagery generated from satellite Synthetic Aperture Radar (SAR) acquisitions. Based on the phase information of received back-scattered radar signals in repeated SAR acquisitions over the same area, it is possible to extract ground surface displacements in the radar line-of-sight. In this analysis, the pre-seismic SAR acquisitions were combined with post-seismic acquisitions to generate the maps of coseismic ground displacements associated with the M_w 6.4 Petrinja earthquake.

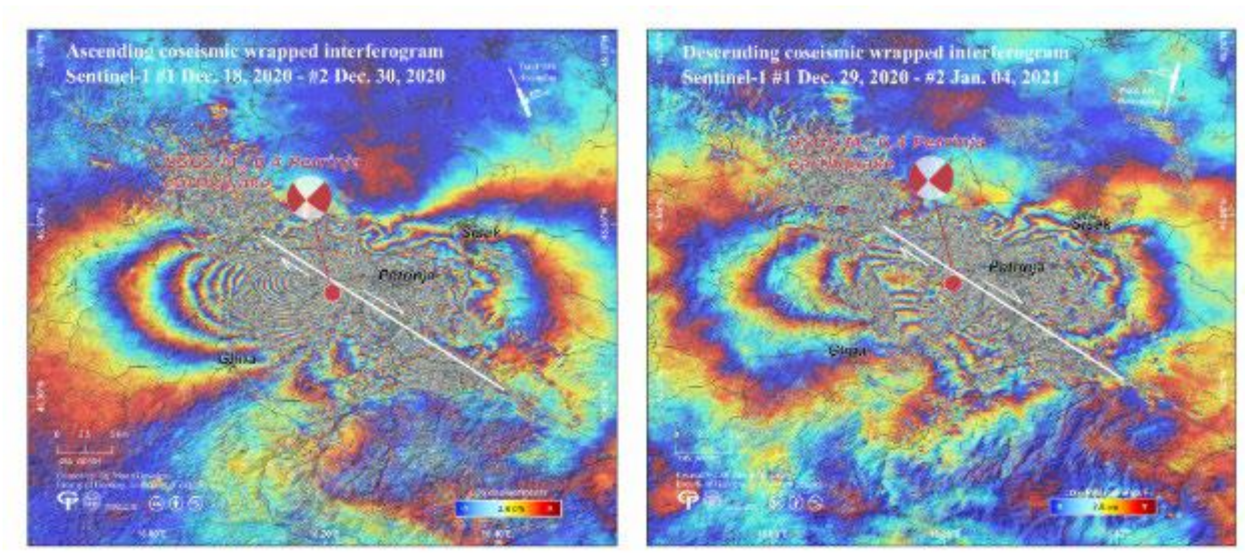

Figure 5.1. Coseismic wrapped interferograms calculated with the data acquired from Sentinel-1 a) ascending and b) descending track. Interferograms show ground displacements wrapped in 2pi modulo (a fringe) in the satellite's line-of-sight direction depicted with white arrows in the right upper image corner. One-color cycle (“fringe”) represents half of the satellite’s wavelength movement of 2.8 cm. The white line marks a potential location, length, and orientation of the activated Petrinja fault. The focal mechanism solution and epicenter location of M_w. 6.4 Petrinja earthquake is shown as red beachball and circle, respectively (adapted from USGS, 2020).

We used Sentinel-1 images acquired on Dec. 18 and Dec. 30 from the ascending orbit track 146 and the images acquired on Dec. 29 and Jan. 04 from the descending orbit track 124 to form an ascending and descending track coseismic interferogram, respectively (**Figure 5.1 a,b**). Coseismic ground deformations can be observed in the form of interferometric fringes (color cycles; red-yellow-green-blue-red), where one fringe represents a ground motion of 2.8 cm (the half of satellite wavelength). A total number of “fringes” multiplied by 2.8 cm gives a maximum ground displacement. The interferograms show a classic strike-slip “butterfly” deformation pattern forming two deformation lobes on each side of the fault (Fialko et al., 2005). The observed deformation pattern points to an NW-SE-oriented fault situated between Petrinja and town Glina. However, the exact surface fault trace cannot be observed in the interferograms due to a high level of decorrelation in the fault's near-field. We suspect that this is due to the shaking of a ground highly saturated with water. The potential location of the Petrinja fault trace is depicted as white and black lines centered in the middle of a ground deformation pattern in **Figure 5.1 a,b,** and **Figure 5.2 a,b,** respectively. The ascending track interferogram shows around 15 fringes west and 11 fringes east of the decorrelation zone corresponding to a maximum displacement of around 40 cm towards the satellite (in NW-direction) and about 31 cm away from the satellite (in SE-direction), respectively. The descending track interferogram shows around six fringes west and ten fringes east, corresponding to a maximum displacement of 18 cm away from the satellite (in NW-direction) and 28 cm towards the satellite (in SE-direction) respectively. Coseismic ground deformations are shown in **Figure 5.2,** as unwrapped interferograms obtained after the unwrapping process, i.e., calculation of absolute interferometric phase values. We consider the observed ground deformation to be almost completely associated with the M_w 6.4 Petrinja earthquake, due to a short period between Sentinel-1 acquisitions and the earthquake. Both interferograms point to a right-lateral motion consistent with a published USGS moment tensor solution.

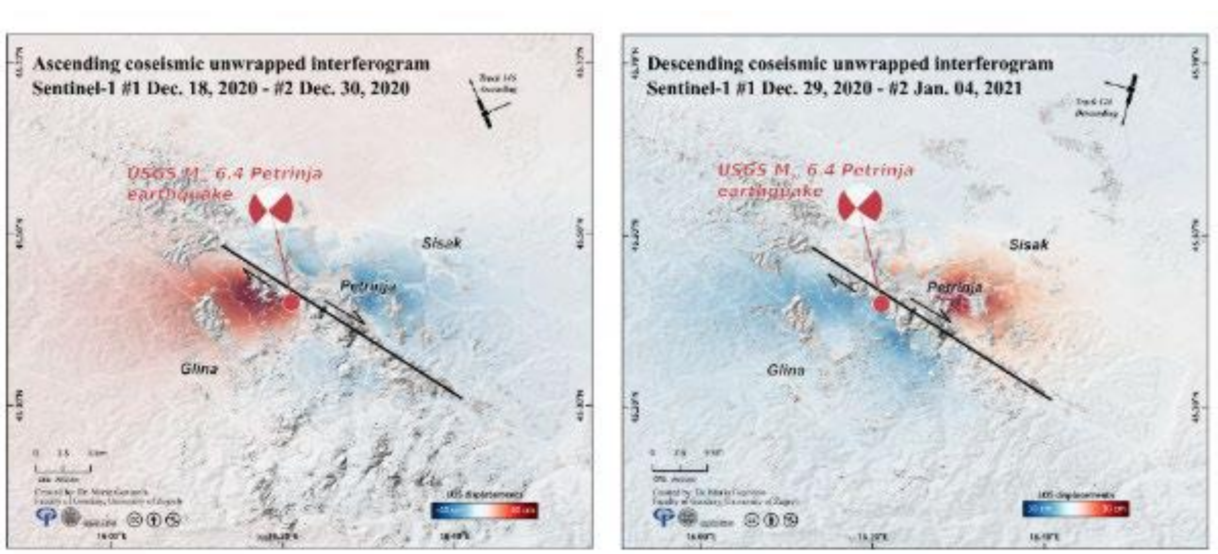

Figure 5.2. Coseismic unwrapped interferograms calculated with the data acquired from Sentinel-1 a) ascending and b) descending track. Unwrapped interferograms show ground movement in the satellite line-of-sight shown in the upper right image corner. Highly decorrelated areas are masked out from the interferograms. The black line marks a potential location, length, and orientation of the activated Petrinja fault. The focal mechanism solution and epicenter location of M_w. 6.4 Petrinja earthquake is shown as red beachball and circle, respectively (source USGS, 2020).

5.2. Surface deformations during past earthquakes strike-slip faults worldwide

One of the most prominent right-lateral strike-slip faults globally is the San Andreas fault (Pacific Plate and North American Plate) which is over 800 miles long and at least 10 miles deep into the Earth's crust (Schulz & Wallace, 2016). The land characteristics of the fault movement appear as long straight escarpments, narrow ridges, and small undrained ponds (Schulz & Wallace 2016). San Andreas' largest recorded strike-slip movements were recorded in the 1906 earthquake (Mw= 7.9) and had an offset of 21 feet (Bray et al., 1994). Recent geological surveys of topographyin California between Cajon Pass and the Salton Sea displayed similar terranes on opposite sides of the fault, showing a potential of over 150 miles of strike-slip movement along the San Andreas fault (Schulz et al., 2016). Wells and Coppersmith (1994) conducted an empirical analysis of 69 field cases of surface fault rupture, finding that the magnitude of the quake and fault type movement exhibited surface displacements of 1 centimeter to at most 10 meters (in Bray et al., 1994). From this field case study, further geotechnical analysis on earthquake fault propagation through soil found that three parameters affect ground deformation: type of fault movement, the inclination of the fault plane, and nature of overlying soil deposit (Bray et al., 1994). In Bray et al. (1994), strike-slip faults tend to follow an almost vertical orientation of the underlying bedrock fault and may spread or "flower" near the ground surface. The movement centralizes above the bedrock, and after the failure occurs, differential displacement localizes to distinct failure planes (Bray et al., 1994). If the soil is ductile, the fault movement will be more significant(Bray et al., 1994). Compared to the normal and reverse faults, strike-slip faulting produces the least amount of subsidiary fault movement and secondary deformation in bedrock due to the differential movement diminishing as the fault propagates up toward the ground surface (Bray etal., 1994). Several physical experiments explained better strike-slip earthquake movements: Tchalenko (1970) comparing Riedel experiment direct shear box of plastic clay with strike-slip fault zones, and Emmons (1969) strike-slip faulting in the sand (after Bray et al., 1994). Field observations and experimental data indicate that both stress characteristics and kinematicconstraints control the behavior of the soil above the bedrock fault movement (Bray et al., 1994). In 1972 Managua earthquake (Mw=6.4) a left-lateral strike-slip fault occurred with approximately3 inches of slip (Rojahn, 1973). The city is on a relatively flat alluvial plain with thick volcanic ash-laden mudflows and thinner bed deposits. Boring reports showed the soil ranges from poorly to well consolidated, with low densities and high porosities (Rojahn, 1973). A massive undergroundconcrete bank vault (that was stronger than the sand and gravel around it) deflected the ruptureout of its normal alignment (Bray et al., 1994). The 2002 Denali seismic event was a right-lateral strike-slip earthquake (Mw=7.9) with several smaller aftershocks occurring seconds afterward (Eberhart-Phillips et al., 2003). The event ruptured three faults (Susitna glacier Fault, Denali Fault, and Totschunda Fault), and horizontal slip deformations were at an average of 5.3 meters (Eberhart-Phillips et al., 2003). Geotechnical reconnaissance was performed after the quake, and35 soil samples were tested from areas (Slana, Nabesna, Tok, Gerstle, Delta, Fielding, and SusitnaRiver) affected by liquefaction (Kayen et al., 2004). The depths of samples ranged from 0 to 2.4 meters and characterized the soils from poorly graded to well-graded sand and gravel, with somesilty sand (Kayen et al., 2004). The 2001 Kokoxili earthquake (Mw = 7.8) in the northeastern edgeof the Tibet plateau recorded the first-time observation of simultaneous events of pure strike-slipand normal faulting (Klinger et al., 2005). The rupture front propagated faster near the surface resulting in tension cracks opening ahead of the shear dislocation and then later disrupted by a propagating strike-slip offset (Klinger et al., 2005). Breaks occurred in alluvial areas of summer floods of seasonal streams using field observations and high-resolution satellite images (Klinger et al., 2005). The 2010 Darwin (Mw=7.1) right-lateral strike-slip earthquake resulted in 4.6 meters of displacement and an average of approximately 2.3 meters across the entire rupture on the Greendale Fault (Cubrinovski et al., 2010). The most severe damages were liquefaction, and historical studies showed that the areas affected were previously river flood plains, lagoon, and estuaries (Cubrinovski et al., 2010). Before this event, the Greendale Fault had not ruptured since the Last Glaciation (Cubrinovski et al., 2010).

References

Bray, D. J., Seed, R. B., Cluff, L.S., Seed, B. H. (1994). *Earthquake fault rupture propagation through soil*. Journal of Geotechnical Engineering, 120(3), p.543–561.

Cubrinovski, M., Russell A. G., Allen, J., Ashford, S., Bowman, E., Bradley, B., Cox, B., Hutchinson, T., Kavazanjian, E., Orense, R., Pender, M., Quigley, M., & Wotherspoon, L. (2010). *Geotechnical Reconnaissance of the 2010 Darfield (Canterbury) Earthquake*. Bulletin of the New Zealand Society for Earthquake Engineering, 43 (4), p.243–320. Available at: https://doi.org/10.5459/bnzsee.43.4.243-320 (Accessed: 8 May 2021)

Eberhart-Phillips, D., Haeussler, P. J., Freymueller, J. T., Frankel, A. D., Rubin, C. M., Craw, P., Ratchkovski, N. A., Anderson, G., Carver, G. A., Crone, A. J., Dawson, T. E., Fletcher, H., Hansen, R., Harp, E. L., Harris, R. A., Hill, D. P., Hreinsdóttir, S., Jibson, R. W., Jones, L. M., Kayen, R., Keefer, D. K., Larsen, C. F., Moran, S. C., Personius, S. F., Plafker, G., Sherrod, B., Sieh, K., Sitar, N., Wallace, W. K. (2003). *The 2002 Denali Fault Earthquake, Alaska: A Large Magnitude, Slip-Partitioned Event*. Science, 300(5622), p1113–18. Available at: https://doi.org/10.1126/science.1082703 (Accessed: 8 May 2021)

Emmons, R. C. (1969). "Strike-slip rupture patterns in sand models." Tectonophysics, 7(1), 71-87.

Fialko, Y., Sandwell, D., Simons, M., Rosen, P. (2005). *Three-dimensional deformation caused by the Bam, Iran, earthquake and the origin of shallow slip deficit*. Nature, 435, p295–299.

Kayen, R., Thompson, E., Minasian, D., Moss, R. E. S., Collins, B. D., Sitar, N., Dreger, D. and Carver, G. (2004). *Geotechnical Reconnaissance of the 2002 Denali Fault, Alaska, Earthquake*. Earthquake Spectra, 20(3), p639–667. Available at: https://doi.org/10.1193/1.1778389 (Accessed: 8 May 2021)

Klinger, Y., Xu, X., Tapponnier, P., Van der Woerd, J., Lasserre, C. and King, G. (2005). *High-Resolution Satellite Imagery Mapping for the Surface Rupture and Slip Distribution of the Mw ~7.8, 14 November 2001 Kokoxili Earthquake, Kunlun Fault, Northern Tibet, China*. Bulletin of the Seismological Society of America, 95(5), p1970–1987.

Rojahn, C. (1973). *Managua, Nicaragua Earthquake of December 23, 1972*. Earthquake Engineering Research Institute Conference Proceedings Vol.1 Supported in part by the National Science Foundation; Cosponsored by Ministry of Public Works of Nicaragua, American Concrete Institute, American Iron and Steel Institute, American Society of Civil Engineers, Association of Engineering Geologists, Seismological Society of America, Structural Engineers Association of California, November 29-30, 1973, San Francisco, California. Oakland: Earthquake Engineering Research Institute.

Schulz, S. S., Wallace, R. E. (2016). *The San Andreas Fault* [Online]. U.S Department of the Interior: U.S. Geological Surveys. Available at: https://pubs.usgs.gov/gip/earthq3/safaultgip.html (Accessed: 8 May 2021)Tchalenko, J. S. (1970). "Similarities between shear zones of different magnitudes." Geol. Soc. Am. Bull., 81(Jun.), 1625-1640

USGS (2020) M 6.4 - 2 km WSW of Petrinja, Croatia. Available at https://earthquake.usgs.gov/earthquakes/eventpage/us6000d3zh/executive. Published 29 December 2020.

Wells, D., and Coppersmith, K. (1994). "New empirical relationships among magnitude, rupture length, rupture width, rupture area and surface displacements." Seism. Soc. Am. Bull., 84(4)